A RGBD-based system for real-time robotic defects detection on sewer networks

L. Merino, D. Alejo, S. Martinez-Rozas and F. Caballero

Service Robotics Laboratory, Universidad Pablo de Olavide, Seville, Spain.
{lmercab,daletei,fcaballero}@upo.es
s.martinez.r@ieee.org

Abstract. In this paper we summarize the automatic defect inspection onboard the sewer inspection ground platform SIAR. We include a general overview of the software and hardware characteristics of our platform, making a special emphasis on the sensing devices and software systems that are used for defect inspection. The main detection algorithm makes use of the a priori knowledge of ideal sections of the sewers that can be found in the Geographic Information Systems (GIS), and uses a variant of the Iterative Closest Point (ICP) algorithm for finding structural and serviceability defects. Then, we describe the software modules that are in charge of storing the alerts found by the detection system and of displaying them to the operator. The whole system has been tested in two field scenarios on different locations of the real sewer network of Barcelona, Spain.

Keywords: Sewer inspection · Defect Detection · Field robotics.

1 Introduction

Sewers represent a very important infrastructure of cities. The state of the sewer network has to be assessed in order to intervene if damages, blockages and other hazards are discovered. This is a labour intensive task. For instance, Barcelona has a 1532 km long network, in which 50% can be visited by operators. Furthermore, sewer inspections require many people to work in risky and unhealthy conditions. Sewers are classified as confined spaces which require special health and safety measures, in addition to other risks present like slippery sections, obstacles or biological risks from the potential contact with waste water.

Including a robotic solution for sewer inspection could thus provide many advantages. First, it would reduce labor risks, as it prevents operators to enter in such spaces, in which health hazards are common. Second, robots can acquire precise data and process it in real-time to perform a 3D-mapping of the environment or to automatically detect structural defects on the environment. Last, the use of such systems can reduce the costs involved in the inspection of sewers.

And thus, there are a wide variety of robotic platforms for sewer inspection already in the market, mainly for pipe inspection (like Alligator, Minigator, Multigator and Flexigator wheeled robots from IBAK or Geolyn's tracked robots

to name a few), but also for larger ones (like ServiceRoboter wheeled solution from Fraunhofer IFF). In this paper, we consider the SIAR robotic solution developed in the frame of the EU Project ECHORD++.

Most of the previous systems are manually operated and relay information for the operator, who performs the inspection. Providing automatic inspection capabilities can reduce inspection times.

Again, most of the available research has been designed for inspecting conventional sewer pipe networks. For example, the KARO system is aimed at analyzing the rings of light projected onto the internal pipe wall so as to detect pipe deformations and obstacles, and detecting leakage using microwave sensors [1]. The PIRAT system classifies defects using a feed-forward neural network classifier, which is trained off-line [2]. Unfortunately, these kind of experimental platforms usually lack of testing in real scenarios: their experimentation is limited to a laboratory replica of the real sewers or a very small part of the real sewer network.

There is also work on automatic problem detection which uses data collected by closed-circuit television (CCTV) systems, such as the early framework proposed in [3]. More recently, neural network and deep learning approaches are becoming more and more common. For example, an automated recognition process for infiltration defects in sewer pipes can be found in [4]. In [5] an optical flow based approach for CCTV camera motion analysis to automatically identify, locate and extract frames of inspection video which likely include defects is presented. Also, the work in [6] uses Hidden Markov models to generate consistent anomaly detection using CCTV. However, the inspection based on CCTV systems is not able to get metric measures to the detected anomalies, they have to infer them by taking into account the cross section of the pipe. Moreover, they lack the flexibility offered by a mobile platform.

To fill this gap, this paper presents a method that is able to automatically detect defects on the sewer network. To this end, our system uses range data available from multiple RGB-D sensors onboard of our SIAR robotic platform, which is presented in Section 2. Furthermore, it is able to distinguish two main classes of defects: structural defects and serviceability defects, as presented in Section 3. In addition, the tools developed to make this information available to the operators in real-time are presented in Section 4. Finally, we tested the system in the real sewer network of Barcelona (see Section 5.2). Section 6 analyzes the results of the system and lists the future challenges and research directions.

2 Overview of the SIAR platform

A new ground robot, the SIAR platform[1], has been developed to tackle the requirements of the sewer inspection application [7]. In this section, we will briefly describe the robotic platform, paying special attention to the sensor payload that is used for the detection of defects on the sewer network.

The SIAR robot is a six-wheeled differential ground platform. The wheel traction system is composed by six sets of independent motors and 260 mm

[1] http://siar.idmind.pt/

(a) (b) (c) (d)

Fig. 1. a) detail of the SIAR platform. b-c) the robot being introduced in the manhole. d) SIAR platform inside the sewer network.

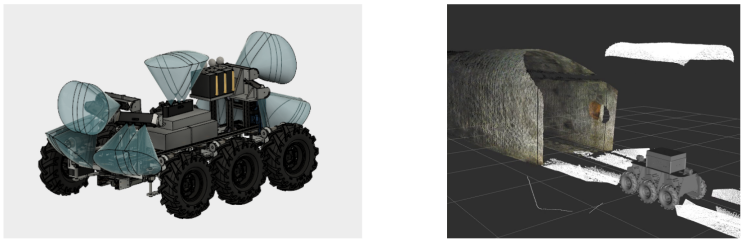

(a) (b)

Fig. 2. (a) The robot carries seven RGB-D cameras. (b) These cameras provide high-resolution 3D point clouds of the environment, used for automatic defect detection.

off-road wheels. Each of these sets has an independent suspension arm that connects to the central robot frame. Due to the specifications of the problem, the robot must be introduced through a manhole, which is noticeably smaller than the width of the tunnels (see Fig. 1-b,c). Furthermore, the robot should negotiate sewer sections and gutters of different widths. For this reason, a width adjustment mechanism has been included so that the robot can adapt to these different structural changes in the working environment.

2.1 Sensor payload for structural inspection

The robot is equipped with a set of navigation and environmental perception sensors. The main element of the sensor payload is a set of seven Orbbec Astra RGB-D cameras[2] that provides visual and depth information. The cameras are placed symmetrically as presented in Fig. 2-a. There are three RGB-D cameras looking forward, three backwards and one upwards. For each direction, the robot has a camera parallel to the ground to detect damage in the tunnel and to illustrate the operator controlling the robot. Additionally, we disposed two cameras facing downwards and sideways to visualize closer range obstacles and defects. The upward facing camera is placed over the center of the robot. This camera is used for detecting flaws in the tunnel dome and for identifying sewer elements

[2] https://orbbec3d.com/product-astra-pro/

such as manholes. Fig. 2-b represents a combined point cloud with the depth information of all cameras. Additionally, we placed a camera on the end-effector of a robotic arm with five degrees of freedom. This camera can be controlled by the operator to obtain closer looks of areas of interest.

For navigation, the robot also uses encoders to control the velocity of the traction motors and an encoder plus a potentiometer to control the position of the platform width actuator. The robot is also equipped with an inertial sensor. The information of these sensors and the RGB-D cameras is used for estimating the position of the robot according to GIS data, as presented in [8].

3 Serviceability and Structural Defects Inspection System

There are two types of problems that are considered by the current inspection system:

- Sewer serviceability inspection: determine when there is debris in the gutters and floor that may obstruct the sewer.
- Structural defects inspection: determine the presence of cracks, fractures, breaks and collapses in the structure of the sewers.

This system uses the 3D input data given by the onboard set of RGB-D cameras of the robot to generate, in real-time, serviceability and/or structural defects alarms that can be displayed in the Control Station for the operator. Furthermore, those alarms are time-stamped and geo-located (by considering the robot localization system), and a report is generated when the mission finishes for mission de-briefing and post-processing.

The processing pipeline of the system is summarized in Fig. 3. We describe the main modules of the system in the following:

1. **Automatic detection of sewer type**: a point cloud is generated by combining information from all cameras. This model is aligned with a database of 3D virtual models of the different section types stored in the robot, according to the drawings of the different sections present in the zone to inspect. The virtual point cloud which contain labels for the different parts of the sewer: gutter, curbs, walls and roof, see Fig. 4-b. The alignment is carried out using the Iterative Closest Point (ICP) algorithm [9]. ICP is initialized by generating the model point clouds in the frame of the cameras, which approximately aligned with the gathered point cloud. The model with the lowest ICP error is selected as the current section type, Fig. 4-a.
2. **Segmentation of sewer elements**: once the virtual model is aligned with the 3D data, the current point cloud is segmented into the different parts of the sewer; that is, each 3D point is classified as either gutter, curbs, walls or roof. Each point of the cloud is labeled according to the label of the closest point in the virtual 3D model of the sewer, which contains this information. Fig. 5 shows the results of the segmentation.

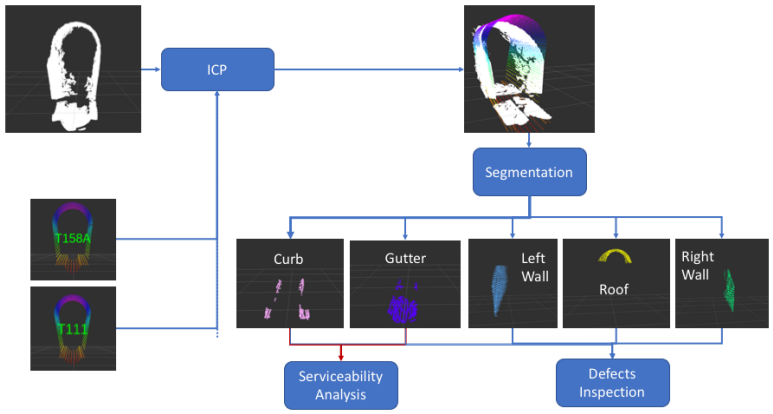

Fig. 3. Main processing pipeline. ICP algorithm is used to estimate (and align) the current section type by comparing the 3D data (in white) with virtual models from the database. Then, the parts related to serviceability (curb and gutter, sill, etc) are segmented from the input point cloud. These parts are analyzed to estimate potential serviceability and structural alarms.

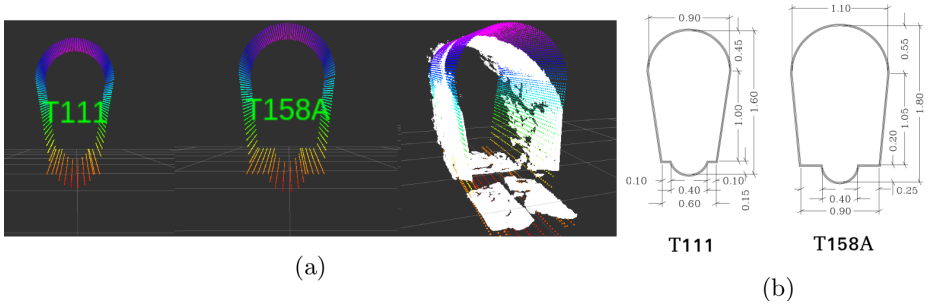

(a) (b)

Fig. 4. a) Measures for Sections T111 and T158A. b) Center and Right: Virtual ideal 3D models for section types T111 and T158A. Right: the current 3D data (white) is aligned using ICP to all the models in the database searching for the one that best fit the data.

3. **Serviceability inspection**: with the information of the two above processes, the serviceability analysis begins. Only the parts corresponding to the gutter, curbs and sill are considered in such analysis. Then, on one hand, the method extracts those points that separate from the model further than a minimum distance, as these points may indicate deviations from the ideal section model, and thus a potential serviceability problem. At the same time, the absolute maximum, minimum and mean height of the 3D points segmented as points of the gutter are computed. This way it is possible to estimate if the gutter could be blocked by comparing with the ideal minimum, maximum and mean height of the gutter. The same is carried out

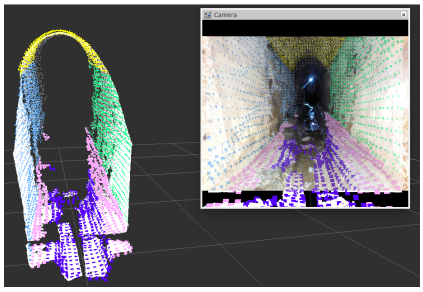

Fig. 5. Point-cloud segmentation. After the alignment with the section, the points are segmented according to the different parts of the sewer. Left: points segmented as gutter (purple), curb (pink), left wall (blue), right wall (green) and roof (yellow). The points projected back on the frontal camera of the robot can be also seen.

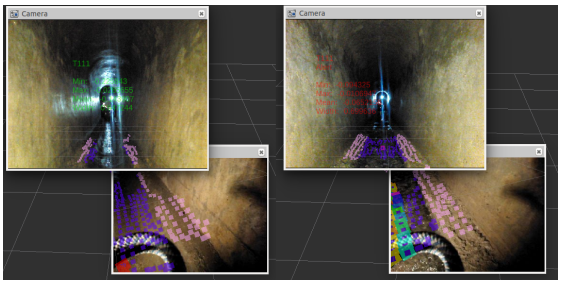

Fig. 6. Left: the serviceability of the gallery is correct. The frontal and down right cameras are shown (there is a down left camera that is not shown for clarity). In green, the absolute values for the height of the gutter are displayed in the frontal image for the operator. In purple and pink, the 3D points corresponding to the gutter and curb respectively. Right: serviceability alarm. The values are displayed in red. Many of the 3D points in the down-right camera (marked as colored points) are detected as departing from the ideal section (the gutter is blocked by debris).

with the curb. As a result, potential alarms are generated (see Fig. 6). A temporal consistency filter is employed to filter out false alarms due to brief misreadings or misalignment of the sensor data.

4. **Automatic structural defects inspection**: structural defects alarms can be raised by estimating the error between the ideal section model and the 3D data gathered by the sensor. This error is estimated by nearest neighbour search between each point in the cloud and the virtual model of the section. The points for which the error is above a threshold are candidates for potential defects. The threshold is user defined, and can be used to balance the size of the defects and the rate of false alarms, but the system is able to detect defects of the order of centimetres. The arm onboard the SIAR platform is equipped with a camera that can be used for close inspection in order to confirm the potential defects highlighted by the module.

4 Graphical User Interface

The information provided by the online Serviceability and Structural Defects Inspection System (see Section 3) can be displayed to the operator in real-time by using a custom made Graphical User Interface (GUI) at the base station. This GUI can operate in the following modes:

- The exploration mode allows the operator to have localization, real-time images, depth information and SIAR prioceptive information (see Fig. 7). This mode is recommended for taking metric measurements.
- The inspection mode (see Fig. 8-a) includes images from the inspection arm camera. It is recommended for navigation and for obtaining details of defects.
- In the mission execution mode the operator can easily get information about the alerts generated during the experiment (see Fig. 8-b).

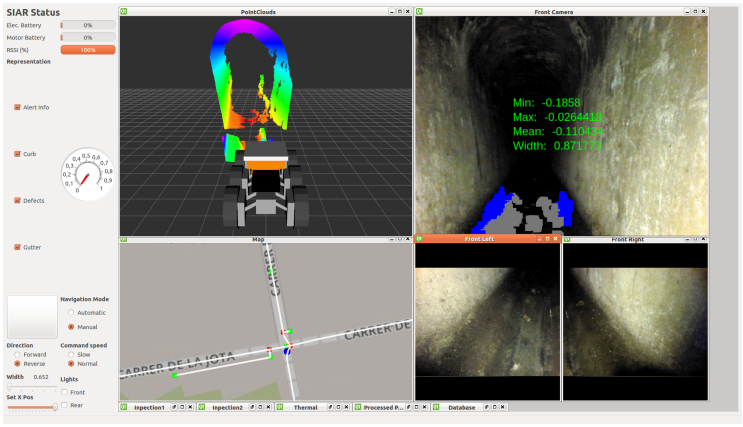

Fig. 7. Exploration view of the GUI. On the leftmost panel, prioceptive information of the platform can be found. On the middle panel, we can see the depth cloud information obtained from the onboard cameras (top) and the localization of the platform with the GIS data (bottom). The rightmost panel shows the composed views of the RGB images from the onboard cameras. The serviceability information is overlayed in green.

The software has been developed as a C++ application for Ubuntu 16.04 and uses the Robotic Operating System (ROS) Kinetic. We make extensive use of the convenient RViz tool [10] for 3D representation and augmented reality purposes. We used the convenient rviz-satellite plugin[3] for GIS representation.

[3] https://github.com/gareth-cross/rviz_satellite

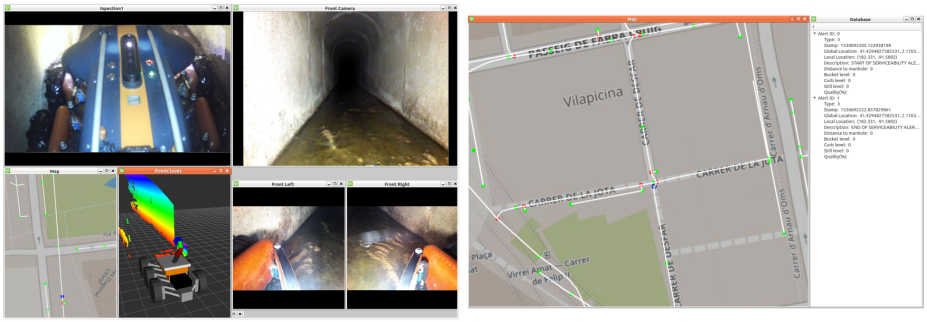

(a) (b)

Fig. 8. (a) Inspection view of the GUI. There is an additional image shown from the camera on the arm (up-left). (b) Mission execution view of the GUI. The generated alerts are shown in the rightmost panel and displayed over the GIS.

5 Experiments

In this section, we present the results obtained from the serviceability and structural defects inspection system in two experiments. These experiments have been carried out in the real sewer network of Barcelona in two different places: Virrei Amat Square and Passeig Garcia Faria.

To perform each experiment, the platform must be introduced through a manhole by the aid of the operators. Once the robot enters the sewer and is left in a stable position to navigate, the platform is configured, controlled and monitored by the base station that is outside the sewer. No operators are required to follow the platform inside the sewers as the inspection routine goes by.

5.1 Experiments at Virrei Amat Square

In this experiment, more than 500 m of sewer galleries were inspected (see Fig. 9). We deployed three repeaters in different manholes along to ensure network connectivity between the SIAR platform and the base station.

During the inspection, four serviceability defects were automatically detected and localized by the platform. In particular, our algorithm detected two main zones where there are very noticeable defects where human intervention would be needed for cleaning purposes.

We will now detail the contents of the four automatically generated defects. For each defect, the detection system generated two alerts: one at the beginning of the problem and another when the serviceability is restored. For each alert, we provide the GPS coordinates, time and the distance to the closest manhole.

Serviceability defect 1: Alerts 1 and 2. Fig. 10-a shows a composition of the three images from the frontal cameras. In this case, there are noticeable sediments on the gutter and in the leftmost curb.

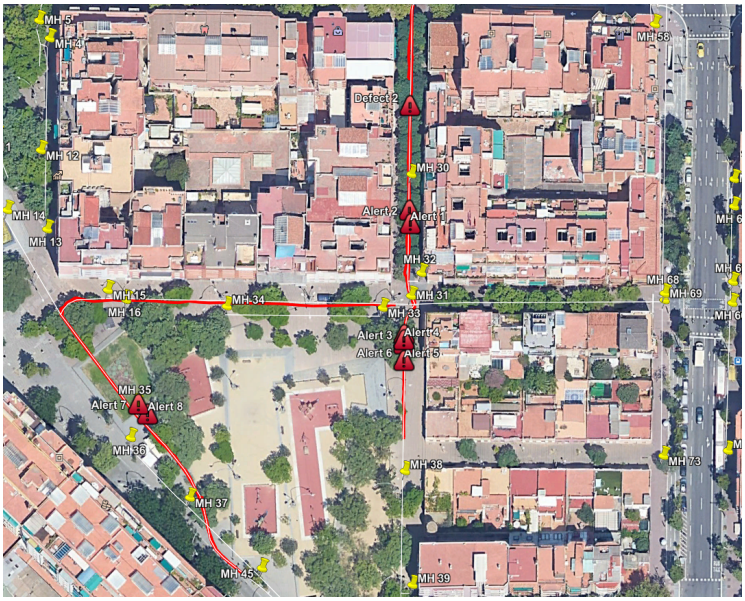

Fig. 9. Inspection report of the experiments at Virrei Amat square. The path followed by the SIAR platform is marked in a red line. The generated alerts by the system are shown in red exclamation marks.

- **Begins:** 41.429 959°N, 2.176 372°E. Local Time: 2018-07-04-10:03:07
  Distance to closest manhole: 17.2 m. Closest manhole: MH 30.
- **Ends:** 41.429 964°N, 2.176 373°E. Local Time: 2018-07-04-10:03:12
  Distance to closest manhole: 17.6 m. Closest manhole: MH 30.

Serviceability defect 2: Alerts 3 and 4. Fig. 10-b presents a composition of the three images from the frontal cameras. In this case, sediments are accumulated in the gutter and they prevent the water from flowing.

- **Begins:** 41.429 397°N, 2.176 346°E. Local Time: 2018-07-04-10:32:44.
  Distance to closest manhole: 10.5 m. Closest manhole: MH 31.
- **Ends:** 41.429 392°N, 2.176 345°E. Local Time: 2018-07-04-10:32:48.
  Distance to closest manhole: 10.8 m. Closest manhole: MH 31.

Serviceability defect 3: Alerts 5 and 6. Fig. 10-c presents a composition of the three images from the frontal cameras. Sediments are accumulated in the gutter and prevent the water from flowing. The accumulated water at the end of the serviceability defect can be found in the video [4].

- **Begins:** 41.429 374°N, 2.176 344°E. Local Time: 04-07-2018-10:33:02.
  Distance to closest manhole: 12.8 m. Closest manhole: MH 31.

[4] https://robotics.upo.es/papers/robot_2019_alert.mp4

(a) (b) (c) (d)

Fig. 10. (a-d): Composed snapshot in Alerts 1-4 in Virrei Amat, respectively.

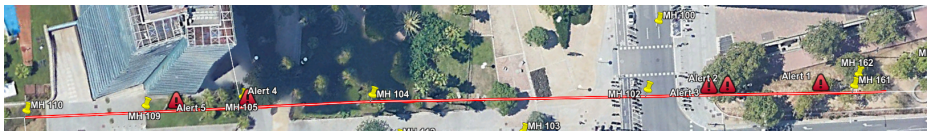

Fig. 11. Inspection report of the experiments at Passeig de Garcia Faria. The localization of the SIAR platform is plotted in a red line. The alerts generated by the system are marked in red exclamation marks.

– **Ends:** 41.429 333°N, 2.176 344°E. Local Time: 2018-07-04-10:33:22.
Distance to closest manhole: 16.7 m. Closest manhole: MH 31.

Serviceability defect 4: Alerts 7 and 8. Fig. 10-d presents a composition of the three images from the rear cameras. We found a noticeable sediment over the rightmost curb and some sediments at the gutter.

– **Begins:** 41.429 209°N, 2.175 506°E. Local Time: 2018-07-04-11:56:21.
Distance to closest manhole: 5.3 m. Closest manhole: MH 35.
– **Ends:** 41.429 097°N, 2.175 630°E. Local Time: 2018-07-04-11:58:07.
Distance to closest manhole: 9.4 m. Closest manhole: MH 37.

5.2 Experiments at Passeig de Garcia Faria - Barcelona

The SIAR platform inspected a 200 m long straight-line sewer during this experiment. Next we detail the defects found by the proposed system. In particular, it found three defects and one structural element that are marked in Fig. 11:

Serviceability defect 1: Alerts 1 and 2. The system detected an anomaly in the serviceability in the first part of the inspected area. In this case, the water covered the complete surface of the floor and thus the anomaly was reported. The obtained data indicates an anomaly in the gutter levels as shown in Fig.12-a.

– **Begins:** 41.407 281°N, 2.218 564°E. Local Time: 2018-12-13-11:57:47.
Distance to closest manhole: 7.4 m. Closest manhole: MH 161.

– **Ends:** 41.407 144°N, 2.218 369°E. Local Time: 2018-12-13-12:02:47.
Distance to closest manhole: 19.3 m. Closest manhole: MH 102.

Structural defect 1: Alert 3. Structural defect 1. Fig. 12-b and 12-b.1 show the visual and 3D representations, respectively. In this case, a noticeable obstacle of 14.4 cm can be found in the rightmost curb.

– Location: 41.407 116°N, 2.218 330°E. Local Time: 2018-12-13-12:08:55.
Distance to closest manhole: 12.2 m. Closest manhole: MH 102.

Structural element 1: Alert 4. The system detected an inlet in one of the sides of the gallery. Fig. 12-c and 12-c.1 show visual and 3D representations of the surroundings of the inlet, respectively. We estimated its height on 19.1 cm, which can be of use for determining if it has been built according to the laws.

– Location: 41.406 434°N, 2.217 364°E. Local Time: 2018-12-13-12:08:55
Distance to closest manhole: 1.1 m. Closest manhole: MH 105.

Structural defect 2: Alert 5. Fig. 12-d and 12-d.1 show visual and 3D representations, respectively. We observe a 7.2 cm tall inlet with its sediments.

– Location: 41.406 327°N, 2.217 217°E. Local Time: 2018-12-13-12:20:01
Distance to closest manhole: 8.9 m. Closest manhole: MH 109.

6 Conclusion

In this paper we have presented a system for automatic defect report generation on the sewer networks. This detection is performed online, and the obtained defects are shown to the operator immediately, which allows to allocate more resources to validate the defect or just gathering more information of interest. The complete system includes the defect detection system that fuses the information of up to 7 RGB-D cameras and a GUI for representing the report in real-time. The system has been demonstrated during the field experiments on the real sewer networks of Barcelona.

The system currently detects automatically potential alarms that are then confirmed by the operator. Future work includes the automatic classification of the detected anomalies and defects as cracks, collapses, structural elements, etc, by using learning approaches. The information of the structural elements can be included as features in the localization system in order to increase the precision of both the localization of the alerts and of the localization of the platform.

References

1. H. Kuntze and H. Haffner: "Experiences with the development of a robot for smart multisensoric pipe inspection", in Proceedings. 1998 IEEE International Conference on Robotics and Automation , vol. 2, pp. 17731778 vol.2, 1998.

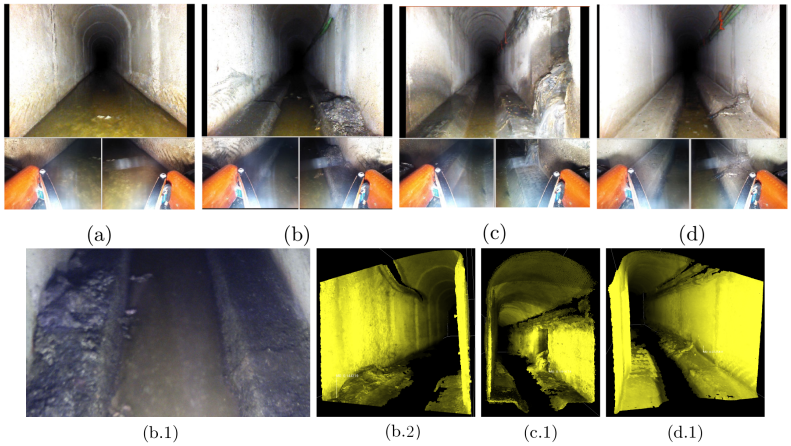

Fig. 12. (a) Composed snapshot in Serviceability Defect 1 of the experiment in Passeig Garcia Faria. (b) Composed snapshot in Structural Defect 1, with an obstacle in the rightmost curb. (b.1) Detail of the obstacle obtained with the arm camera (b.2) Obtained 3D mesh in Structural Defect 1 (the obstacle is on the left). (c) Composed snapshot in Structural Element 1. There are some sediments under an inlet on the rightmost curb. (c.1) 3D mesh in Structural Element 1. (d) Composed snapshot in Structural Defect 1. It is on the rightmost curb and is composed by sediments that come from an inlet. (d.1) 3D mesh in Structural Defect 2.

2. R. Kirkham, P. D. Kearney, K. J. Rogers, and J. Mashford: "Pirata system forquantitative sewer pipe assessment". In The International Journal of Robotics Research, vol. 19, no. 11, pp. 10331053, 2000.
3. O. Moselhi and T. Shehab:"Automated detection of surface defects in water and sewer pipes". Automation in Construction, vol. 8, no. 5, pp. 581 588, 1999.
4. T. Shehab and O. Moselhi:"Automated detection and classification of infiltration in sewer pipes". J. of Infrastructure Systems , vol. 11, no. 3, pp. 165171, 2005.
5. M. R. Halfawy and J. Hengmeechai:Integrated vision-based system for automated defect detection in sewer closed circuit television inspection videos". Journal of Computing in Civil Engineering, vol. 29, no. 1, p. 04014024, 2015.
6. S. Moradi and T. Zayed: Real-Time Defect Detection in Sewer Closed Circuit Television Inspection Videos , pp. 295307. 2017.
7. ECHORD++, Utility infrastructures and condition monitoring for sewer network. robots for the inspection and the clearance of the sewer network in cities. http://echord.eu/public/wp-content/uploads/2015/11/20141218Challenge-BriefUrbanRobotics.pdf, 2014, 2014.
8. D. Alejo, F. Caballero, and L. Merino: Rgbd-based robot localization in sewer networks. In 2017 IEEE/RSJ International Conference on Intelligent Robots and Systems (IROS), pp. 40704076, Sept 2017.
9. P. J. Besl and N. D. McKay. A method for registration of 3d shapes. IEEE Trans. Pattern Analysis and Machine Intelligence , vol. 14, no. 2, pp. 239256, 1992.
10. H. Kam, S.-H. Lee, T. Park, and C.-H. Kim, Rviz: a toolkit for real domain data visualization, Telecommunication Systems, vol. 60, pp. 19, 10 2015.